J. Am. Chem. Soc. 1987, 109, 4584-4592

Ferromagnetic Behavior of Linear Chain Charge Transfer Complexes. Structural and Magnetic Characterization of Decamethylferrocenium Hexacyanobutadienide (1:1): $[Fe(C_5Me_5)_2]^{\bullet+}[C_4(CN)_6]^{\bullet-}$

Joel S. Miller,*[1a] Jian H. Zhang,[1b] and William M. Reiff*[1b]

Contribution from the Department of Chemistry, Northeastern University, Boston, Massachusetts 02115, and the Central Research and Development Department, E. I. du Pont de Nemours and Co., Inc., Experimental Station E328, Wilmington, Delaware 19898.

Received November 26, 1986

Abstract: The reaction of $Fe(C_5R_5)_2$ (R = H, Me) and hexacyanobutadiene results in the formation of a charge transfer complex of $[Fe(C_5R_5)_2]^{\bullet+}[C_4(CN)_6]^{\bullet-}$ composition. Crystals of $[Fe(C_5Me_5)_2]^{\bullet+}[C_4(CN)_6]^{\bullet-}$ belong to the centrosymmetric $P2_1/n$ space group [a = 10.783 (5) Å, b = 8.719 (3) Å, c = 14.266 (4) Å, β = 91.22 (3)°, Z = 2, V = 1340.9 Å^3]. The unit cell is comprised of alternating $S = {}^1/_2$ cations and $S = {}^1/_2$ anions aligned along the a axis. Each cation has a staggered D_{5d} symmetry with the bond distances ~0.01 Å greater than those previously reported for $[Fe(C_5Me_5)_2]^{\bullet+}$. The average Fe–C, C–C, and C–Me separations are 2.104, 1.447, and 1.516 Å, respectively. The $S = {}^1/_2$ $[C_4(CN)_6]^{\bullet-}$ planar anion is disordered. A model attributing the disorder to equivalent contributions of two trans orientations enabled the refinement of the structure to R = 6.2% and R_w = 8.3%. The deconvoluted anions possessing local C_2 symmetry have essentially equivalent distances (±0.01 Å from the average values): CC—CC = 1.43 Å, C—CCC = 1.31 Å, $(C\text{—}CN)_{int}$ = 1.65 Å, C≡N = 0.92 Å, $(C_4\text{—}CN)_{exo}$ = 1.52 Å, $(C_4\text{—}CN)_{endo}$ = 1.64 Å, $(C{\equiv}N)_{exo}$ = 1.093 Å, and $(C{\equiv}N)_{endo}$ = 0.85 Å. The C–C–C_3, CC–C–C, CCC–C–$(CN)_{endo}$, and NC–C–CN angles (±1°) are 143, 105, 119, and 127°, respectively. As a consequence of the imposed disorder model the sp cyano carbons are substantially nonlinear with 167 ± 1° observed for the four essentially parallel C—C≡N angles and 150 ± 3° for the exo nitriles. The intrachain Fe^{III}–Fe^{III} distance is 10.783 Å, whereas the interchain Fe^{III}–Fe^{III} separations less than the intrachain spacing are 8.719, 9.865, and 10.030 Å. The dihedral angle between the planar anion and the C_5 ring is 26.4°, and the average separation is ~3.7 Å. Above 100 K the magnetic susceptibility obeys the Curie–Weiss expression (Θ = +35 K) and the charge transfer salt has dominant ferromagnetic interactions. Magnetic saturation occurs for all fields measured, i.e., 30 G < H < 50 kG, and at 1.91 K the saturation magnetization is 1.77×10^4 emu G/mol. The magnetic behavior is as expected for a 3-D ferromagnet. Above 10 K this complex exhibits classical ferrocenium singlet ^{57}Fe Mössbauer spectra [isomer shift, δ = 0.422 mm/s relative to iron foil; line width, $\Gamma \sim$ 0.35 mm/s]. Below 10 K zero-field Zeeman split spectra are evident and fully resolved at 6 K. At 1.68 K the spectrum corresponds to splitting by an internal field of 449 kG. On the basis of the susceptibility and Mössbauer data, the ordering temperature is 7.5 ± 0.5 K. In contrast the unmethylated ferrocenium analogue, $[Fe(C_5H_5)_2]^{\bullet+}[C_4(CN)_6]^{\bullet-}$, does not exhibit zero-field Zeeman split ^{57}Fe Mössbauer spectra [δ(1.6 K) = 0.555 mm/s, Γ(1.6 K) ~ 0.70 mm/s] and the magnetic susceptibility above 2 K obeys the Curie–Weiss expression (Θ = −3.4 K) with μ_{eff} = 3.34 μ_B consistent with isolated $S = {}^1/_2$ cations and $S = {}^1/_2$ anions.

Linear chain, 1-D, complexes containing strong acceptors have been shown over the past quarter of a century to frequently exhibit unusual electronic, particularly electrical properties.[2] In 1979 we reported[3] on the metamagnetic behavior observed for the 1-D phase of $[Fe(C_5Me_5)_2]^{\bullet+}[TCNQ]^{\bullet-}$ [TCNQ = 7,7,8,8-tetracyano-*p*-quinodimethane]. Since metamagnetism involves field dependent switching from the antiferromagnetic state to a low-lying ferromagnetic state, we have deliberately sought to prepare charge transfer complexes possessing a ferromagnetic ground state. Thus, we have undertaken the systematic study of the structure–function relationship between salts comprised of primarily metallocenium cations and planar polycyano acceptors with the goal of elucidating the electronic and steric requirements for the stabilization of the ferromagnetic state. Previously we have reported that $[Fe(C_5Me_5)_2]^{\bullet+}$ salts of 2,3-dichloro-4,5-dicyanobenzoquinoneide,[4] $[DDQ]^{\bullet-}$, $[C_3(CN)_5]^-$,[5b] $[C(CN)_3]^-$,[6] [*p*-$(NC)_2C_6H_4C(O)CN]^-$,[7] $[FeCl_4]^-$,[8] $[FeBr_4]^-$,[9] are paramagnetic above 4 K. Utilizing the tetracyanoethylenide, $[TCNE]^{\bullet-}$, anion as the $[Fe(C_5Me_5)_2]^{\bullet+}$ salt we have demonstrated the occurrence of ferromagnetic ground-state behavior in a charge-transfer salt.[5] With our observation of meta- and ferromagnetic behavior in 1-D charge-transfer complexes, and the theoretical encouragement supplied by McConnell[10,11] that substances of this structure type possessing either cations or anions with an accessible triplet (e^2) excited state capable of mixing with the ground state and stabilizing ferromagnetic coupling,[12] we are continuing to prepare new materials that exhibit ferromagentic coupling. Specifically we aim to prepare complexes with higher transition temperatures, greater stability under ambient conditions, and the ability to form large single crystals enabling the detailed study of the physical properties on oriented single crystals. Herein we report on the

---

(1) (a) DuPont Co. (Contribution No. 4325). (b) Northeastern University.

(2) For a detailed overview, see the proceedings of the recent series of international conferences: (a) Pecile, C.; Zerbi, G.; Bozio, R.; Girlando, A., (Eds. *Mol. Cryst. Liq. Cryst.* **1985**, 117-121. (b) Comes, R.; Bernier, P.; Andre, J. J.; Rouxel, J., *Eds. Phys. (Paris) Collogue* **1983**, 44-C3. (c) Epstein, A. J.; Conwell, E. M., Eds. *Mol. Cryst. Liq. Cryst.* **1981**, 77, 79, 82, 83, 85; **1982**, 86. (d) Carneiro, K., Ed. *Chem. Scr.* **1981**, 17. (e) Bartsic, S.; Bjelis, A.; Cooper, J. R.; Leontic, B. A., Eds. *Lecture Notes in Phys.* **1979**, 95 and 96. (f) Miller, J. S.; Epstein, A. J., Eds. *Ann. N.Y. Acad. Sci.* **1978**, 313.

(3) Candela, G. A.; Swartzendruber, L.; Miller, J. S.; Rice, M. J. *J. Am. Chem. Soc.* **1979**, *101*, 2755-2756.

(4) (a) Gebert, E.; Reis, A. H., Jr.; Miller, J. S.; Rommelmann, H.; Epstein, A. J. *J. Am. Chem. Soc.*, **1982**, *104*, 4403-4410. (b) Miller, J. S.; Krusic, P. J.; Dixon, D. A.; Reiff, W. M.; Zhang, J. H.; Anderson, E. C.; Epstein, A. J. *J. Am. Chem. Soc.* **1986**, *108*, 4459-4466.

(5) (a) Miller, J. S.; Calabrese, J. C.; Epstein, A. J.; Bigelow, R. W.; Zhang, J. H.; Reiff, W. M. *J. Chem. Soc., Chem. Commun.* **1986**, 1026-1028. (b) Miller, J. S.; Calabrese, J. C.; Rommelmann, H.; Chittipeddi, S. R.; Zhang, J. H.; Reiff, W. M.; Epstein, A. J. *J. Am. Chem. Soc.* **1987**, *109*, 769-781.

(6) Dixon, D. A.; Calabrese, J. C.; Miller, J. S. *J. Am. Chem. Soc.* **1986**, *108*, 2582-2588.

(7) Miller, J. S.; Reiff, W. M.; Zhang, J. H.; Preston, L. D.; Reis, A. H., Jr.; Gebert, E.; Extine, M.; Troup, J.; Dixon, Epstein, A. J.; Ward, M. D. *J. Phys. Chem.*, in press.

(8) Reiff, W. M.; Zhang, J. H.; Calabrese, J. C.; Miller, J. S., manuscript in preparation.

(9) Reiff, W. M.; Zhang, J. H.; Miller, J. S., manuscript in preparation.

(10) McConnell, H. M. *Proc. Robert A. Welch Found. Chem. Res.* **1967**, *11*, 144-145.

(11) Breslow, R. *Pure Appl. Chem.* **1982**, *54*, 927-938. Breslow, R.; Jaun, B.; Klutz, R. Q.; Xia, C.-Z. *Tetrahedron* **1982**, *38*, 863-867.

(12) Miller, J. S.; Epstein, A. J. *J. Am. Chem. Soc.*, in press.

0002-7863/87/1509-4584$01.50/0

preparation and ferromagnetic properties of $[Fe(C_5Me_5)_2]^{\bullet+}[C_4(CN)_6]^{\bullet-}$ (1:1).[13]

Experimental Section

$[Fe(C_5Me_5)_2]^{\bullet+}[C_4(CN)_6]^{\bullet-}$ was prepared from $Fe(C_5Me_5)_2$ (Strem Chemical Co.) and hexacyanobutadiene. Webster's route[14] to hexacyanobutadiene was utilized with the modification that the product was extracted with hot dichloromethane. $[Fe(C_5Me_5)_2]^{\bullet+}[C_4(CN)_6]^{\bullet-}$ was prepared in an inert atmosphere glovebox via reaction of decamethylferrocene (200 mg; 0.61 mmol) dissolved in 20 mL of hot acetonitrile with 125 mg (0.61 mmol) of hexacyanobutadiene also in 20 mL of MeCN. After refrigeration at −25 °C overnight the product (268 mg; 83%) was collected via vacuum filtration. Anal. Calcd for $C_{30}H_{30}FeN_6$: C, 67.92; H, 5.70; Fe 10.53; N, 15.85. Found C, 67.98; H, 5.94; N, 15.43. Infrared spectra (Nujol): ν(C≡N) 2168 (m), 2185 (s, 2207 (w, and 2220 (w) cm^{-1}. The spectra are in agreement with those previously reported for Na^+ and $[Et_4N]^+[C_4(CN)_6]^{\bullet-}$.[14,15]

$[Fe(C_5H_5)_2]^{\bullet+}[C_4(CN)_6]^{\bullet-}$ was prepared from and hexacyanobutadiene (120 mg, 0.59 mmol) in an inert atmosphere glovebox via reaction with ferrocene (Strem Chemical Co.) (110 mg; 0.59 mmol) dissolved in 2 mL of hot acetonitrile. After refrigeration at −25 °C overnight 152 mg of the product (66%) was collected via vacuum filtration. Anal. Calcd for $C_{20}H_{10}FeN_6$: C, 61.56; H, 2.58; N, 21.54. Found: C, 61.66; H, 2.67; N, 21.12. Infrared spectra (Nujol): 2178 (sh) 2193 (s), 2219 (s) cm^{-1}. Crystals suitable for single-crystal X-ray diffraction could not be grown.

X-ray Data Collection and Reduction.[16] The original sample was recrystallized from 1,2-dichloroethane. Many (Ca. 20) crystals were examined before a crystal of reasonable quality was obtained. A green prismatic crystal having approximate dimensions of 0.20 × 0.20 × 0.30 mm was mounted on a glass fiber with its long axis roughly parallel to the ϕ axis of the goniometer. Preliminary examination and data collection were performed with MoK_α radiation (λ = 0.71073 Å) on an Enraf-Nonius CAD4 computer controlled κ-axis diffractometer equipped with a graphite crystal, incident beam monochromator.

Cell constants and an orientation matrix for data collection were obtained from least-squares refinement, using the setting angles of 25 relfections in the range $3 < \Theta < 8°$, measured by the computer-controlled diagonal-slit method of centering. The monoclinic cell parameters and calculated volume are a = 10.783 (5) Å, b = 8.719 (3) Å, c = 14.266 (4) Å, β = 91.22 (3)°, V = 1340.9 $Å^3$. For $Z = 2$ and molecular weight of 530.46 daltons the calculated density is 1.31 g/cm^3. As a check on crystal quality, ω scans of several intense reflections were measured; the width at half-height was 0.30° with a take-off angle of 2.8°, indicating good crystal quality. From the systematic absences [$0k0$: $k = 2n + 2$; $h0l$: $h + l = 2n + 1$] and subsequent least-squares refinement the space group was determined to be $P2_1/n$.

The data were collected at −106 ± 1 °C with use of the ω–Θ scan technique. The scan rate varied from 2 to 20°/min (in ω). The variable scan rate allows rapid data collection for intense reflections where a fast scan rate is used and assures good counting statistics for weak relfections where a range (in deg) was determined as a function of Θ to correct for the separation of the $K\alpha$ doublet.[17] The scan width is 0.7 + 0.350 tan θ. Moving-crystal, moving-counter background counts were made by scanning an additional 25% above and below this range. Thus, the ratio of peak counting time to background counting time was 2:1. The counter aperture was also adjusted as a function of θ. The horizontal aperture width ranged from 2.0 to 2.5 mm; the vertical aperture was set to 2.0 mm. The diameter of the incident beam collimator was 0.7 mm, and the crystal-to-detector distance was 21 cm. For intense reflections an attenuator was automatically inserted in front of the detector; the attenuator factor was 20.7.

A total of 1926 reflections were collected of which 1121 were unique and not systematically absent. As a check on crystal and electronic stability three standards remained constant within experimental error throughout data collection. No decay correction was applied.

Lorentz and polarization corrections were applied to the data. The linear absorption coefficient is 6.1 cm^{-1} for Mo $K\alpha$ radiation and no absorption correction was made. An extinction correction was not necessary. Intensities of equivalent reflections were averaged. The agreement factors for the averaging of the 1219 observed and averaged reflections was 6.4% based on intensity and 4.3% based on F_o.

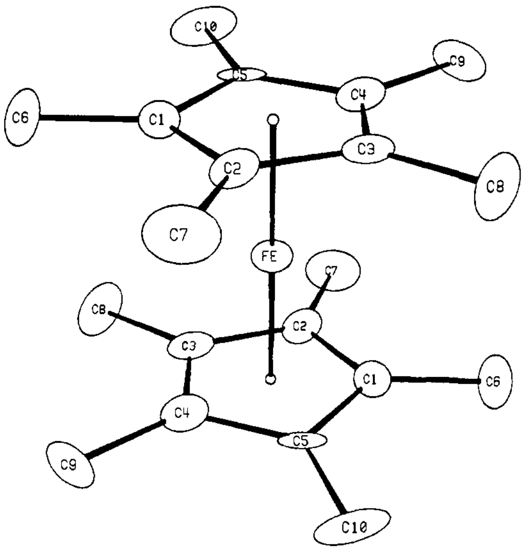

Figure 1. Atom labeling for the $[Fe(C_5Me_5)_2]^{\bullet+}$ cation.

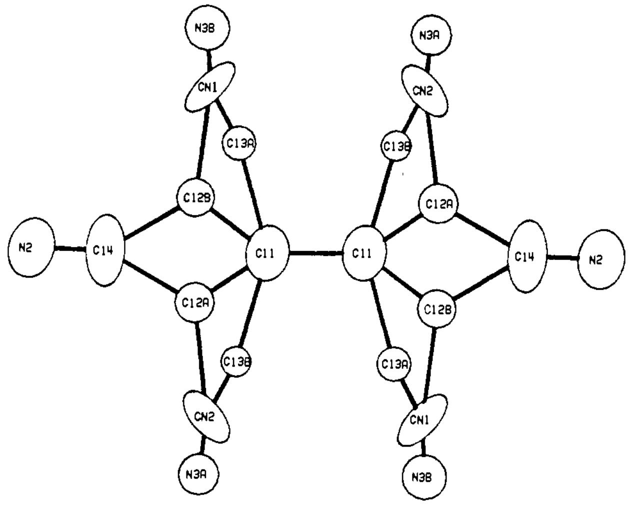

Figure 2. Atom labeling for the disordered pair of $[C_4(CN)_6]^{\bullet-}$ anions, I and II.

X-ray Refinement and Solution. The structure was solved by using the Patterson heavy-atom method which revealed the position of the Fe atom. The remaining atoms were located in succeeding difference Fourier syntheses. The Fe atom lies on a crystallographic inversion center at the origin and the pentamethylcyclopentadienyl ligand is ordered (Figure 1); however, the hexacyanobutadienide anion is disordered. The anion lies on the inversion center at $(0, {}^1/_2, {}^1/_2)$ and the disorder can be explained as a twofold disorder created by rotation along the C11–C11 bond (Figure 2). The atoms labeled with A and B suffixes were refined at 50% occupancy. In many cases the atoms of the two orientations were superimposed or could not be resolved as separate atoms. Figure 2 depicts the two orientations and the proposed disorder scheme. The "half" atoms were refined isotropically and the remaining atoms were refined with anisotropic thermal parameters. Hydrogen atoms were not included in the calculations. The structure was refined in full-matrix least-squares where the function minimized $\sum w(|F_o| - |F_c|)^2$ and the weight w is defined as $4F_o^2/\sigma^2(F_o)^2$. The standard deviation on intensities, $\sigma(F_o^2)$, is defined as $[S^2(C + R^2B) + (pF_o^2)^2]/L_p^2$, where S is the scan rate, C is the total integrated peak count, R is the ratio of the scan time to background counting time, B is the total background count, L_p is the Lorentz–polarization factor, and the parameter p (set to 0.060) is a factor introduced to downweight intense reflections. Scattering factors were taken from Cromer and Waber.[18] Anomalous dispersion effects were included in F_c,[19] the values for $\Delta f'$ and $\Delta f''$ were those of Cromer.[20]

---

[13] A 1-D 2:1 salt can also be prepared: (a) Miller, J. S.; Dixon, D. A. *Science* **1987**, *235*, 871–873. (b) Miller, J. S.; Dixon, D. A.; Calabrese, J. C., manuscript in preparation.

[14] Webster, O. *J. Am. Chem. Soc.* **1964**, *86*, 2898–2902.

[15] A detailed spectroscopic and structural analysis of $[C_4(CN)_6]^n$ (n = 0, 1−, 2−) is the subject of another paper.[13b]

[16] Molecular Structure Corporation (College Station, TX); TEXRAY is a trademark of MSC.

[17] *CAD4 Operations Manual*; Enraf-Nonius, Delft, 1977.

[18] Cromer, D. T.; Waber, J. T. *International Tables for X-Ray Crystallography*; The Kynoch Press: Birmingham, England, 1974; Vol. IV, Table 2.2B.

[19] Ibers, J. A.; Hamilton, W. C. *Acta Crystallog.* **1964**, *17*, 781.

[20] Cromer, D. T. *International Tables for X-Ray Crystallography*; The Kynoch Press: Birmingham, England, 1974; Vol. IV, Table 2.3.1.

Table I. Positional and Thermal Parameters[a] and Their Estimated Standard Deviations[b,c] for $[Fe(C_5Me_5)_2][C_4(CN)_6]$

atom	*x*	*y*	*z*	*β*(1,1)	*β*(2,2)	*β*(3,3)	*β*(1,2)	*β*(1,3)	*β*(2,3)
Fe	0.0000	0.0000	0.0000	0.0027 (2)	0.0078 (3)	0.00245 (9)	0.0010 (6)	−0.0004 (3)	0.0008 (4)
N2	0.100 (1)	0.071 (1)	0.6086 (7)	0.011 (1)	0.017 (2)	0.0083 (8)	−0.004 (3)	−0.005 (2)	0.005 (2)
C1	0.1721 (9)	0.091 (1)	0.0448 (7)	0.003 (1)	0.009 (2)	0.0033 (6)	0.002 (3)	−0.001 (1)	0.000 (2)
C2	0.1512 (9)	−0.057 (1)	0.0875 (7)	0.001 (1)	0.009 (2)	0.0039 (6)	0.003 (2)	−0.002 (1)	0.001 (2)
C3	0.1376 (9)	−0.171 (1)	0.0145 (7)	0.002 (1)	0.009 (2)	0.0047 (7)	0.001 (3)	0.002 (2)	−0.001 (2)
C4	0.1481 (9)	−0.092 (1)	−0.0737 (7)	0.001 (1)	0.013 (2)	0.0039 (6)	−0.002 (3)	0.000 (2)	0.001 (2)
C5	0.1718 (9)	0.068 (1)	−0.0562 (7)	0.001 (1)	0.012 (2)	0.0032 (6)	−0.001 (2)	0.000 (1)	0.002 (2)
C6	0.1947 (11)	0.239 (1)	0.0954 (8)	0.008 (1)	0.008 (2)	0.0054 (7)	−0.002 (3)	−0.003 (2)	−0.007 (2)
C7	0.1492 (10)	−0.088 (1)	0.1924 (7)	0.006 (1)	0.020 (2)	0.0026 (6)	0.003 (3)	−0.000 (2)	0.006 (2)
C8	0.1175 (11)	−0.341 (1)	0.0283 (9)	0.007 (1)	0.003 (2)	0.0090 (9)	−0.002 (3)	−0.002 (2)	0.002 (2)
C9	0.1423 (10)	−0.168 (1)	−0.1712 (7)	0.005 (1)	0.021 (2)	0.0028 (6)	0.005 (3)	0.000 (2)	−0.009 (2)
C10	0.1936 (10)	−0.192 (1)	−0.1282 (7)	0.007 (1)	0.015 (2)	0.0039 (6)	−0.003 (3)	0.004 (2)	0.011 (2)
C11	0.0168 (10)	−0.426 (1)	0.5177 (9)	0.002 (1)	0.015 (2)	0.0080 (9)	−0.006 (3)	−0.002 (2)	0.002 (2)
C14	0.0705 (11)	0.181 (1)	0.5786 (11)	0.006 (1)	0.014 (2)	0.0124 (11)	−0.002 (3)	0.000 (2)	0.013 (3)
CN1	0.0079 (12)	0.430 (2)	0.6978 (8)	0.012 (2)	0.023 (3)	0.0037 (7)	−0.009 (4)	−0.007 (2)	0.011 (2)
CN2	0.0713 (11)	0.246 (1)	0.3835 (9)	0.004 (1)	0.009 (2)	0.0098 (9)	−0.002 (3)	0.001 (2)	−0.009 (2)

atom	*x*	*y*	*z*	*B*, Å²	atom	*x*	*y*	*z*	*B*, Å²
N3A	0.092 (2)	0.207 (2)	0.332 (1)	3.7 (4)	C12B	0.034 (2)	0.348 (3)	0.597 (2)	3.2 (5)
N3B	0.010 (2)	0.462 (2)	0.755 (1)	4.3 (5)	C13A	0.006 (2)	0.443 (2)	0.633 (1)	2.5 (5)
C12A	0.046 (2)	0.287 (3)	0.497 (2)	3.4 (5)	C13B	0.051 (2)	0.320 (2)	0.425 (1)	1.7 (4)

[a] The form of the anisotropic thermal parameter is the following: $\exp[-(\beta(1,1)h' + \beta(2,2)k' + \beta(3,3)l' + \beta(1,2)hk + \beta(1,3)hl + \beta(2,3)kl)]$. [b] Estimated standard deviations in the least significant digits are shown in parentheses. [c] Atoms with "A" and "B" suffixes were refined at 50% occupancy.

Table II. General Temperature Factor Expressions,[a] *B*'s for $[Fe(C_5Me_5)_2][C_4(CN)_6]$

	B(1,1)	*B*(2,2)	*B*(3,3)	*B*(1,2)	*B*(1,3)	*B*(2,3)	B_{eqv}
Fe	1.25 (9)	2.38 (9)	2.00 (8)	0.2 (1)	−0.13 (8)	0.2 (1)	1.88 (4)
C1	1.4 (5)	2.6 (5)	2.7 (5)	0.4 (5)	−0.2 (5)	0.0 (4)	2.2 (3)
C2	0.5 (5)	2.8 (6)	3.2 (5)	0.5 (4)	−0.5 (4)	0.3 (4)	2.2 (3)
C3	0.8 (5)	2.6 (5)	3.8 (5)	0.1 (5)	0.5 (5)	−0.3 (5)	2.4 (3)
C4	0.7 (5)	4.0 (6)	3.2 (5)	−0.3 (5)	0.1 (5)	0.1 (5)	2.6 (3)
C5	0.3 (5)	3.5 (6)	2.6 (5)	−0.2 (4)	0.1 (4)	0.6 (4)	2.1 (3)
C6	3.6 (6)	2.5 (5)	4.4 (6)	−0.4 (5)	−0.8 (5)	−1.7 (5)	3.5 (3)
C7	2.9 (6)	6.0 (7)	2.1 (5)	0.6 (6)	−0.1 (5)	1.5 (5)	3.7 (3)
C8	3.3 (6)	1.0 (5)	7.3 (8)	−0.3 (5)	−0.7 (6)	0.5 (5)	3.9 (3)
C9	2.5 (6)	6.3 (7)	2.3 (5)	0.9 (6)	0.1 (5)	−2.2 (5)	3.7 (3)
C10	3.4 (6)	4.6 (6)	3.2 (5)	−0.6 (6)	1.2 (5)	2.6 (5)	3.7 (3)
C11	1.0 (5)	4.5 (6)	6.5 (8)	−1.1 (6)	−0.5 (5)	0.6 (6)	4.0 (3)
C14	2.9 (7)	4.3 (7)	10.1 (9)	−0.3 (6)	−0.1 (7)	3.1 (7)	5.8 (4)
CN1	5.7 (7)	7.1 (8)	3.0 (5)	−1.7 (7)	−2.1 (6)	2.6 (5)	5.3 (3)
CN2	2.0 (6)	2.8 (6)	8.0 (7)	−0.3 (5)	0.3 (6)	−2.3 (6)	4.3 (3)
N2	4.9 (6)	5.0 (6)	6.8 (6)	−0.8 (5)	−1.4 (5)	1.2 (5)	5.6 (3)

[a] The form of the anisotropic thermal parameter is $\exp[-0.25[h'a'B(1,1) + k'b'B(2,2) + l'c'B(3,3) + 2hkabB(1,2) + 2hlacB(1,3) + 2klbcB(2,3)]$ where *a*, *b*, and *c* are reciprocal lattice constants.

Only the 711 reflections having intensities greater than 3.0 times their standard deviation were used in the refinements. The final cycle of refinement included 166 variable parameters and converged (largest parameter shift was 0.10 times its esd) with unweighted, *R*, and weighted, R_w, agreement factors of

$$R = \sum||F_o| - |F_c||/\sum|F_o| = 0.062$$

$$R_w = [\sum w(|F_o| - |F_c|)^2/\sum wF_o^2]^{1/2} = 0.083$$

The standard deviation of an observation of unit weight was 2.06. The highest peak in the final difference Fourier had a height of 0.48 e/Å³ and was located in the region of the disordered hexacyanobutadienide anion. It was less than 50% the height of the disordered carbon atoms (i.e., "half-carbons") located in the previous map, and the estimated error based on ΔF[21] is 0.11. Plots of $\sum w(|F_o| - |F_c|)^2$ vs. $|F_3|$, reflection order in data collection, sin Θ/λ, and various classes of indices showed no unusual trends. All calculations were performed on a PDP-11/60 based TEXRAY[16] system.

^{57}**Fe Mössbauer Spectroscopy.** Zero-field Mössbauer spectra were determined by using a conventional constant acceleration spectrometer with a 50 mCurie ^{57}Co source electroplated onto the surface and annealed into the body of the 6 μm thick foil of high-purity rhodium in a hydrogen atmosphere. The details of cryogenics, temperature control, etc, have been described previously.[22]

Magnetic Measurements. The magnetic susceptibility was determined for polycrystalline samples over the applied field range of 1.66–5.10 kG by using a Faraday balance at Northeastern University.[22] Additional very low field (30 G) susceptibility and field dependence of magnetization (30 G to 50 kG) were determined by using the SHE "SQUID" magnetometer at the Francis Bitter National Magnet Laboratory. On the basis of the usage history the remnant field has been estimated to be as high as 10 G.

Results and Discussion

Crystal Structure. The monoclinic unit cell is comprised of a unique cation and a disordered anion. The fractional coordinates/anisotropic thermal parameters, general temperature factors, interatomic distance, and angles, as well as weighted least square planes, are located in Tables I–V, respectively. Atom labeling for the cation can be found in Figure 1.

$\mathbf{[Fe(C_5Me_5)_2]^{\bullet+}}$ is an ordered staggered D_{5d} ion possessing distances essentially equivalent to those previously reported for the cation. The average Fe–C, C–C, and C–Me separations of 2.104, 1.447, and 1.516 Å, respectively, are, however, ~0.01 Å larger than those previously reported.[5b] The Fe–C$_5$ ring centroid is 1.707 Å, which is slightly larger (0.007 Å) than previously reported.[5b]

$\mathbf{[C_4(CN)_6]^{\bullet-}}$'s detailed structure is reported for the first time.[15] Analogous to the structures of the $[Fe(C_5Me_5)_2]^{\bullet+}$ salts of $[DDQ]^{\bullet-}$,[4a] $[TCNQ]^{\bullet-}$,[7,23] $[TCNE]^{\bullet-}$,[5] and $[C_3(CN)_5]^{\bullet-}$,[5b] the planar $[C_4(CN)_6]^{\bullet-}$ radical anion is sandwiched between parallel

---

(21) Cruickshank, D. W. *Acta Crystallog.* **1949**, *2*, 154.

(22) Cheng, C.; Reiff, W. M. *Inorg. Chem.* **1977**, *16*, 2097.

(23) Miller, J. S.; Reis, A. H., Jr.; Gebert, E.; Ritsko, J. J.; Salaneck, W. R.; Kovnat, L.; Cape, T. W.; Van Duyne, R. P. *J. Am. Chem. Soc.* **1979**, *101*, 7111–7112.

Table III. Bond Distances[a] (Å) for $[Fe(C_5Me_5)_2][C_4(CN)_6]$

atom 1	atom 2	distance	atom 1	atom 2	distance	atom 1	atom 2	distance
Fe	C1	2.106 (8)	C2	C3	1.446 (10)	C12A	C13B	1.06 (2)
Fe	C1	2.106 (8)	C2	C7	1.523 (11)	C12A	C14	1.51 (2)
Fe	C2	2.092 (8)	C3	C4	1.440 (11)	C12A	CN2	1.68 (2)
Fe	C2	2.092 (8)	C3	C8	1.511 (11)	C12B	C13A	1.02 (2)
Fe	C3	2.112 (8)	C4	C5	1.445 (11)	C12B	C14	1.53 (2)
Fe	C3	2.112 (8)	C4	C9	1.539 (11)	C12B	CN1	1.63 (2)
Fe	C4	2.092 (9)	C5	C10	1.511 (11)	C13A	CN1	0.93 (2)
Fe	C4	2.092 (9)	C11	C11	1.43 (2)	C13A	N3B	1.74 (2)
Fe	C5	2.120 (9)	C11	C12A	1.29 (2)	C13B	CN2	0.91 (2)
Fe	C5	2.120 (9)	C11	C12B	1.33 (2)	C13B	N3A	1.72 (2)
C1	C2	1.447 (11)	C11	C13A	1.66 (2)	C14	N2	1.093 (11)
C1	C5	1.455 (11)	C11	C13B	1.65 (2)	CN1	N3B	0.86 (2)
C1	C6	1.495 (11)	C12A	C12B	1.54 (3)	CN2	N3A	0.837 (15)

[a] Numbers in parentheses are estimated standard deviations in the least significant digits.

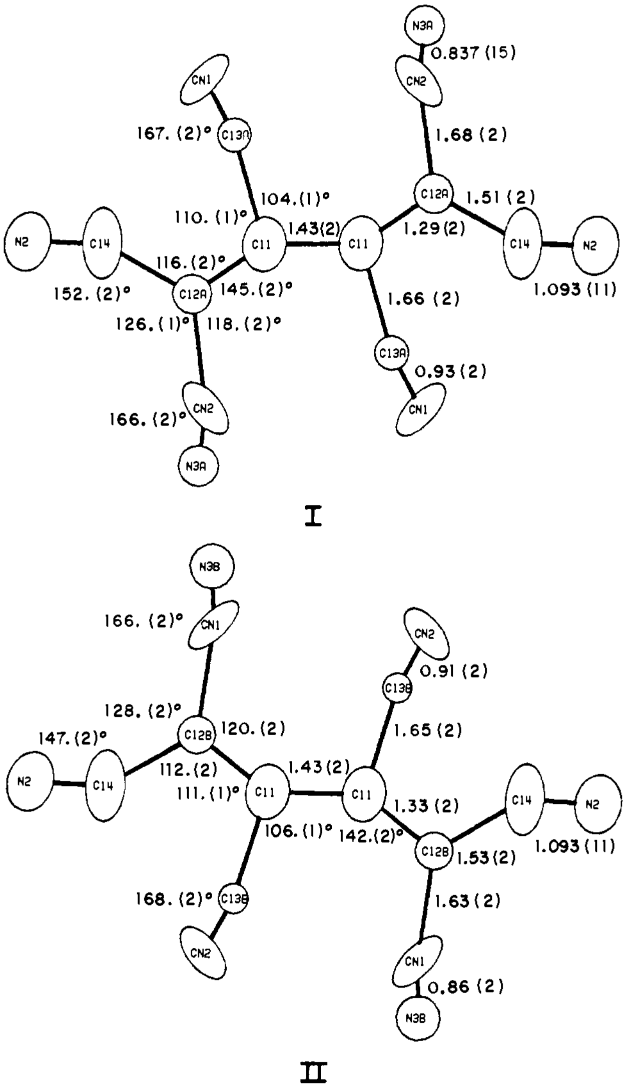

Figure 3. Deconvoluted $[C_4(CN)_6]^{\cdot-}$'s I (a) and II (b).

C_5 rings on two adjacent cations. Unlike these other substances the anion in this structure is orientationaly disordered.[24] The raw refined anion structure (Figure 2) can be deconvoluted via a disorder model where the anion can exist in either of two orientations, i.e., the anions can be eclipsed or flipped so that although the central CC–CC bonds align the CC–CC framework takes on the opposite sense. The *CC–CC* is effectively flipped by 72° in the disordered form. As noted in Figure 2 the central CC and exo cyano C experience minimal positional disorder; however, the length and C—C≡N angles are poorly resolved. With use of this model a pair of essentially equivalent $[C_4(CN)_6]^{\cdot-}]$ anions each possessing local C_2 symmetry can be refined (Figure 3). The bond distances and angles for each anion, designated I and II, are tabulated in Table VI and shown in Figure 3. Metric agreement between I and II is either ±0.01 Å or ±1°. Clearly, the C—C≡N angles deviate substantially from linearity. The exo nitrile angle is 150° whereas the four parallel nitriles average 167°. The former deviation is not surprising upon viewing Figure 2. As summarized in Table VI these distances can be contrasted with those reported for the nonplanar *cis*-hexacyanobutadienide dianion.[25] The skeletal central C–C and endo and exo C–CN bonds are 0.04, 0.24, and 0.11 Å shorter than that observed for the radical anion, whereas the C–CCC is 0.13 Å longer. The C≡N bonds for the dianion exhibit the expected lengths ranging from 1.147 to 1.160 Å, which is 0.06–0.3 Å longer than that observed in the mo-

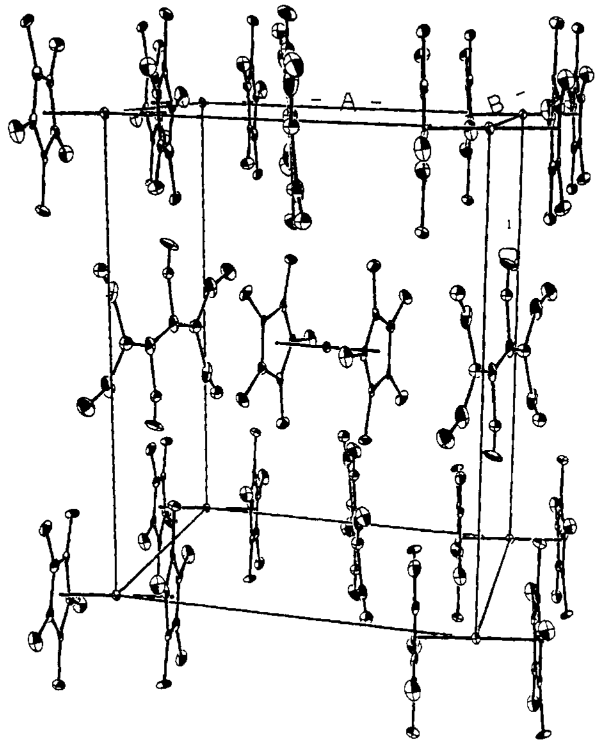

Figure 4. Unit cell of $[Fe(C_5Me_2]^{\cdot+}C_4(CN)_6]^{\cdot-}$.

---

(24) Disordered $[C_4(CN_6]^{\cdot-}$ ions have reported for $[Me_2C_2S_2C_2]_2$, Me_4TTF, 1:1 and 2:1 salts. They utilize a disorder model different than ours and they report substantially different bond distances; however, since they used Cu Kα at room temperature and do not report details of the structure or angles we do not have the basis to properly compare the structures. Katayama, C.; Honda, M.; Kumagai, H.; Tanaka, J.; Saito, G.; Inokuchi, H. *Bull. Chem. Soc. Jpn.* **1985**, *58*, 2272–2278. Saito, G.; Enoki, J.; Inokuchi, H.; Kumagai, H.; Katayama, C.; Tanaka, J. *Mol. Cryst. Liq. Cryst.* **1985**, *120*, 345–348. Tanaka, J.; Katayama, C.; Kumagai, H.; Saito, G.; Enoki, T.; Inokuchi, H. *Mol. Cryst. Liq. Cryst.* **1985**, *125*, 223–232.

(25) Maverick, E.; Goldish, E.; Bernstein, J.; Truebood, K. N.; Swamainathan, S.; Hoffmann, R. *J. Am. Chem. Soc.* **1972**, *94*, 3364–3370.

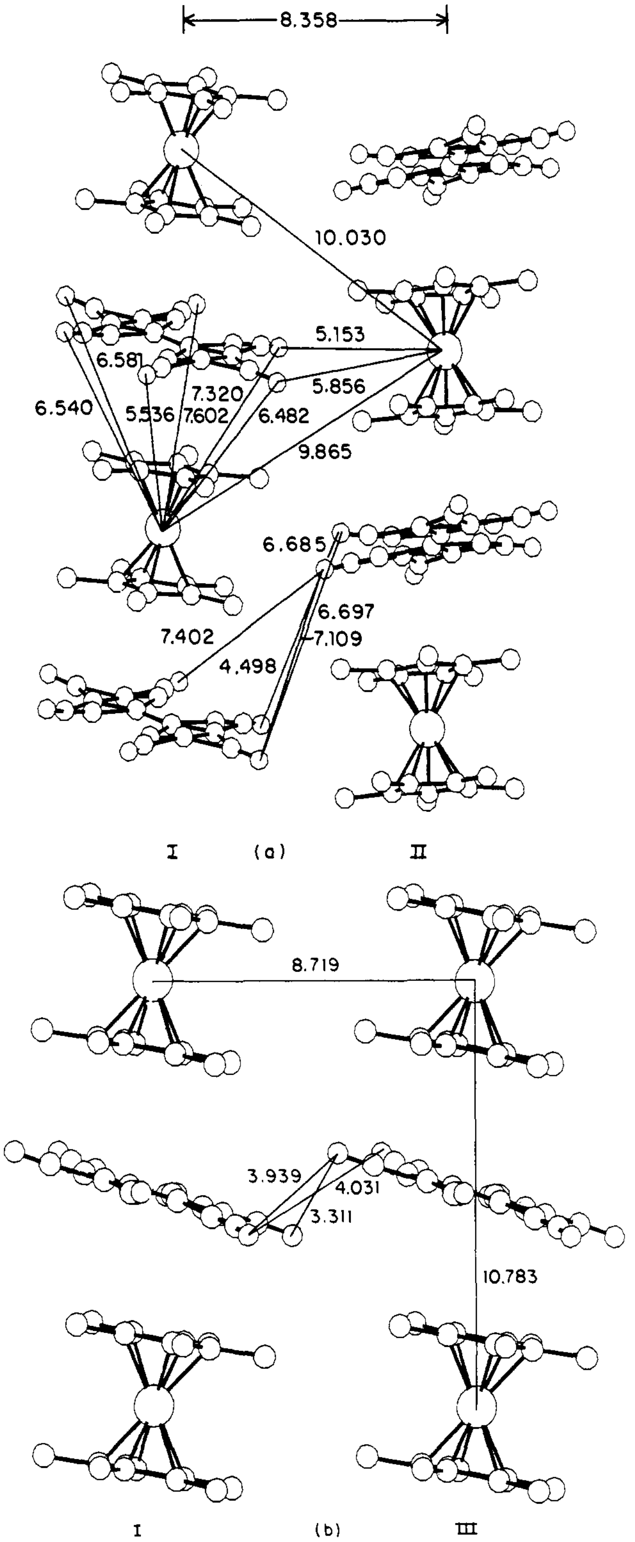

Figure 5. Out-of-registry interactions between chains I-II (a) and in-registry interactions between chains I-III (b).

noanion. The poor quality of the C≡N bond lengths in the monoanion no doubt results from the disorder. The substantial deviations in the angles arise from the twisted structure imposed by the endo nitrile interactions and are not discussed. The C—C≡N angles, however, are linear, i.e., 177.8-178.6°.[15]

Solid-State Structure. The solid is comprised of segregated chains of alternating $S = {}^1/_2$ cations and $S = {}^1/_2$ anions (Figures 4 and 5). The intrachain Fe^{III}-Fe^{III} distance is 10.783 Å, which is 0.37 Å longer than that observed for ferromagnetic [Fe(C$_5$Me$_5$)$_2$][TCNE].[5b] This undoubtedly arises from the 26.4° canting of the anion plane with respect to the C$_5$ ring. There are two independent chain–chain interactions, I–II and I–III, separated by 8.358 and 8.719 Å, respectively. Chains I–II possess parallel chains that are out-of-registry by $a/2$ and have interchain Fe–Fe separations of 9.865 and 10.030 Å, whereas chains I–III are in-registry and have a Fe–Fe distance of 8.719 Å. There are no significant interion separations less than the sum of the van der Waals radii. The planar C$_5$ ring and planar [C$_4$(CN)$_6$]$^{\cdot-}$ ion form a dihedral angle of 26.4°. A view of the unit cell based on ordered anions can be seen in Figure 4.

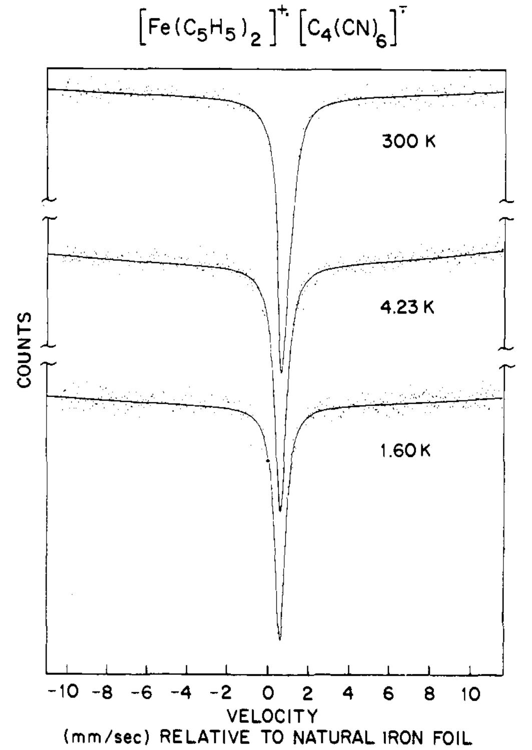

Figure 6. ^{57}Fe Mössbauer spectra of [Fe(C$_5$H$_5$)$_2$]$^{\cdot+}$[C$_4$(CN)$_6$]$^{\cdot-}$ as a function of temperature for $1.60 < T \leqslant 300$ K.

Mössbauer Spectroscopy. The temperature dependence of the ^{57}Fe Mössbauer spectra of [Fe(C$_5$Me$_5$)$_2$]$^{\cdot+}$[C$_4$(CN)$_6$]$^{\cdot-}$ and [Fe(C$_5$H$_5$)$_2$]$^{\cdot+}$[C$_4$(CN)$_6$]$^{\cdot-}$ were obtained between 1.6 and 300 K. For the ferrocenium salt a singlet characteristic of Fe^{III}[26] was observed [isomer shift, δ (line width, Γ) 0.438 (0.555 (0.631), and 0.555 mm/s (0.701 mm/s), was 300, 4.23, and 1.60 K, respectively], Figure 6, and no evidence for unusual solid-state interactions exists. This is confirmed via analysis of the magnetic properties of this charge-transfer complex (vide infra). The steady increase in Γ suggests the possibility of incipient (single ion) slow paramagnetic relaxation and the onset of Zeeman splitting blow 1.6 K.

Above 10 K the ^{57}Fe Mössbauer spectra of the decamethylferrocenium system also exhibit a narrow singlet typical of ferrocenium cations[4b,5b,7,26] (Table VII). Below ~9 K, however, spectral broadening and hyperfine splitting are evident with near full resoltuion, (Figure 7). Saturation is achieved at ~7.5 K. The Mössbauer parameters as a function of temperature are given in Table VII. Below 7.5 K the spectral transitions further sharpen and ultimately lead to a single Zeeman pattern corresponding to a unique iron site. The overall spectroscopic behavior is more reminiscent of slow paramagnetic relaxation as observed for ferromagnetic [Fe(C$_5$Me$_5$)$_2$][TCNE][5b] or metamagnetic [Fe(C$_5$Me$_5$)$_2$][TCNQ][7] than of cooperataive 3-D ordering phenomena. Thus, the internal field, H_i, is relatively temperature independent and the intensity of the central absorption gradually disappears. (The magnetic susceptibility measurements strongly suggests a 3-D ordering temperature of ~7.5 K, vide infra.) The

---

[26] Bagus, P. S.; Walgren, U. I.; Ahmolf J. *J. Phys. Chem.* **1976**, *64*, 2324–2334. Ernst, R. D.; Wilson, D. R.; Herber, R. H. *J. Am. Chem. Soc.* **1984**, *106*, 1646–1650.

Table IV. Table of Bond Angles[a] (deg) for $[Fe(C_5Me_5)_2][C_4(CN)_6]$

atom 1	atom 2	atom 3	angle	atom 1	atom 2	atom 3	angle	atom 1	atom 2	atom 3	angle
C1	Fe	C1	180.0	C4	Fe	C5	40.1 (3)	C11	C12A	C13B	89 (2)
C1	Fe	C2	40.3 (3)	C5	Fe	C5	180.0	C11	C12A	C14	116 (2)
C1	Fe	C2	139.7 (3)	Fe	C1	C2	69.3 (5)	C11	C12A	CN2	118 (2)
C1	Fe	C3	67.9 (3)	Fe	C1	C5	70.4 (5)	C12B	C12A	C13B	144 (2)
C1	Fe	C3	112.1 (3)	Fe	C1	C6	127.2 (6)	C12B	C12A	C14	60 (1)
C1	Fe	C4	67.7 (3)	C2	C1	C5	107.3 (8)	C12B	C12A	CN2	171 (2)
C1	Fe	C4	112.3 (3)	C2	C1	C6	126.2 (7)	C13B	C12A	C14	154 (2)
C1	Fe	C5	40.3 (3)	C5	C1	C6	126.4 (9)	C13B	C12A	CN2	29 (1)
C1	Fe	C5	139.7 (3)	Fe	C2	C1	70.4 (5)	C14	C12A	CN2	126 (1)
C1	Fe	C2	139.7 (3)	Fe	C2	C3	70.6 (5)	C11	C12B	C12A	53 (1)
C1	Fe	C2	40.3 (3)	Fe	C2	C7	127.0 (6)	C11	C12B	C13A	89 (2)
C1	Fe	C3	112.1 (3)	C1	C2	C3	109.1 (7)	C11	C12B	C14	112 (2)
C1	Fe	C3	67.9 (3)	C1	C2	C7	125.4 (0)	C11	C12B	CN1	120 (2)
C1	Fe	C4	112.3 (3)	C3	C2	C7	125.5 (8)	C12A	C12B	C13A	141 (3)
C1	Fe	C4	67.7 (3)	Fe	C3	C2	69.1 (5)	C12A	C12B	C14	59 (1)
C1	Fe	C5	139.7 (3)	Fe	C3	C4	69.2 (5)	C12A	C12B	CN1	172 (2)
C1	Fe	C5	40.3 (3)	Fe	C3	C8	127.1 (6)	C13A	C12B	C14	159 (2)
C2	Fe	C2	180.0	C2	C3	C4	107.0 (8)	C13A	C12B	CN1	31 (1)
C2	Fe	C3	40.2 (3)	C2	C3	C8	126.5 (8)	C14	C12B	CN1	128 (2)
C2	Fe	C3	139.8 (3)	C4	C3	C8	126.6 (9)	C11	C13A	C12B	53 (2)
C2	Fe	C4	67.3 (3)	Fe	C4	C3	70.7 (5)	C11	C13A	CN1	167 (2)
C2	Fe	C4	112.7 (3)	Fe	C4	C5	71.0 (6)	C11	C13A	N3B	174 (2)
C2	Fe	C5	67.4 (3)	Fe	C4	C9	127.0 (6)	C12B	C13A	CN1	113 (2)
C2	Fe	C5	112.6 (3)	C3	C4	C5	109.2 (8)	C12B	C13A	N3B	125 (2)
C2	Fe	C3	139.8 (3)	C3	C4	C9	125.7 (2)	CN1	C13A	N3B	13 (1)
C2	Fe	C3	40.2 (3)	C5	C4	C9	125.0 (8)	C11	C13B	C12A	51 (1)
C2	Fe	C4	112.7 (3)	Fe	C5	C1	69.3 (5)	C11	C13B	CN2	168 (2)
C2	Fe	C4	67.3 (3)	Fe	C5	C4	68.9 (5)	C11	C13B	N3A	177 (2)
C2	Fe	C5	112.6 (3)	Fe	C5	C10	127.4 (6)	C12A	C13B	CN2	117 (2)
C2	Fe	C5	67.4 (3)	C1	C5	C4	127.5 (3)	C12A	C13B	N3A	127 (2)
C3	Fe	C3	180.0	C1	C5	C10	126.3 (9)	CN2	C13B	N3A	10 (1)
C3	Fe	C4	40.1 (3)	C4	C5	C10	127.2 (8)	C12A	C14	C12B	61 (1)
C3	Fe	C4	139.9 (3)	C11	C11	C12A	145 (2)	C12A	C14	N2	152 (2)
C3	Fe	C5	67.5 (3)	C11	C11	C12B	142 (2)	C12B	C14	N2	147 (2)
C3	Fe	C5	112.5 (3)	C11	C11	C13A	104 (1)	C12B	CN1	C13A	35 (1)
C3	Fe	C4	139.9 (3)	C11	C11	C13B	106 (1)	C12B	CN1	N3B	166 (2)
C3	Fe	C4	40.1 (3)	C12A	C11	C12B	72 (1)	C13A	CN1	N3B	154 (2)
C3	Fe	C5	112.5 (3)	C12A	C11	C13A	110 (1)	C12A	CN2	C13B	34 (1)
C3	Fe	C5	67.5 (3)	C12A	C11	C13B	40 (1)	C12A	CN2	N3A	166 (2)
C4	Fe	C4	180.0	C12B	C11	C13A	38 (1)	C13B	CN2	N3A	159 (3)
C4	Fe	C5	40.1 (3)	C12B	C11	C13B	111 (1)	C13B	N3A	CN2	11 (1)
C4	Fe	C5	139.9 (3)	C13A	C11	C13B	149 (1)	C13A	N3B	CN1	13 (1)
C4	Fe	C5	139.9 (3)	C11	C12A	C12B	55 (1)				

[a] Numbers in parentheses are estimated standard deviations in the least significant digits.

origin of this nonclassical behavior is likely related to the magnetic one-dimensional nature of this and related $\cdots D^{\bullet +}A^{\bullet -}D^{\bullet +}A^{\bullet -}D^{\bullet +}A^{\bullet +}\cdots$ materials based on decamethylferrocenium.[27] This type of system can support moving domain boundary effects[29] or solitons has recently been shown to be responsible for line width broadening and splitting in the Mössbauer spectra of some chain antiferromagnets of Fe(II) at temperatures above the critical temperature.[30] For a traditional three-dimensional magnet, the temperature of the onset of line width broadening (or resolved Zeeman splitting) and that of "true" 3-D order as determined via susceptibility, heat capacity, or neutron diffraction measurements are nearly equal. It does not seem reasonable that the broadening observed herein is a slow, single ion relaxation effect in nature. Ferrocenium ions have a spin doublet ground state that normally exhibits a fully allowed, rapid relaxation effect between its $m_s = \pm{}^1/_2$ component Zeeman states.[4b] Slow relaxation broadening effects for low spin Fe(III) are typically only observed for high dilution (increasing spin–spin relaxation times) and then usually in the presence of external magnetic fields.[4b]

Magnetic Susceptibility. $\mathbf{[Fe(C_5Me_5)_2]^{\bullet +}[C_4(CN)_6]^{\bullet -}}$. High-temperature Faraday balance susceptibility measurements (50–300 K) show that $[Fe(C_5Me_5)_2]^{\bullet +}[C_4(CN)_6]^{\bullet -}$ obeys the Curie–Weiss law, $\chi_M^{-1} = C/(T - \Theta)$, with $\Theta = +35$ K.[31] The value of Θ suggests a dominant ferromagnetic interaction. In view of the structure and previous work on the $[TCNE]^{\bullet -}$ analogue[5b,27–29] this is consistent with 1-D ferromagnetic coupling along the $\cdots D^{\bullet +}A^{\bullet -}D^{\bullet +}A^{\bullet -}D^{\bullet +}A^{\bullet -}\cdots$ chains and a weaker 3-D interchain ferromagnetic interaction at low temperatures. Alternatively, by analogy with $[Fe(C_5Me_5)_2][TCNQ]^3$ for which θ is also positive, but an order of magnitude lower in value, i.e., $\theta = +3$ K, the interchain interaction may be antiferromagnetic. That is χ_M vs. T exhibits a classical antiferromaganetic maximum at low temperatures for sufficiently small values of H_0; however, above a critical field (1600 G for the latter material) a high moment state thought to correspond to the decoupling of the antiferromagnetic coupled chains occurs, i.e., metamagnetic behavior is observed. In order to test these possibilities (3-D ground-state ferromagnetism vs. antiferromagnetism), a variety of susceptibility measurements were made. Marked field dependent susceptibility is observed below 6 K (Figure 8). This is essentially coincident with the onset of magnetic hyperfine splitting of the Mössbauer spectra (vide infra). The susceptibility data and Mössbauer spectra suggest an ordering temperature of 7.5 ± 0.5 K.

The qualitative nature of the observed field dependence, i.e., χ_M, decreasing as H_0 increases, is consistent with the usual demagnetization effects for a 3-D ferromagnetic ground-state system. More sensitive, much lower field measurements (30 G, Figure 9) were made with a SQUID magnetometer as part of a search for an antiferromagnetic maximum in χ_M. This was done in consideration of the possibility that $[Fe(C_5Me_5)_2][C_4(CN)_6]$ could be a metamagnet as suggested for $[Fe(C_5Me_5)_2][TCNQ]^3$ but with a much smaller critical field. As can be seen χ_M appears to level off for $H_0 = 30$ G at the limiting temperature (~1.8 K)

---

(27) Above 16 K the susceptibility of $[Fe(C_5Me_5)_2][TCNE]$ fits a 1-D Heisenberg model with ferromagnetic coupling and 3-D behavior is noted for temperatures of order of the Curie temperature, $T_c \sim 4.8$ K.[5b,28]

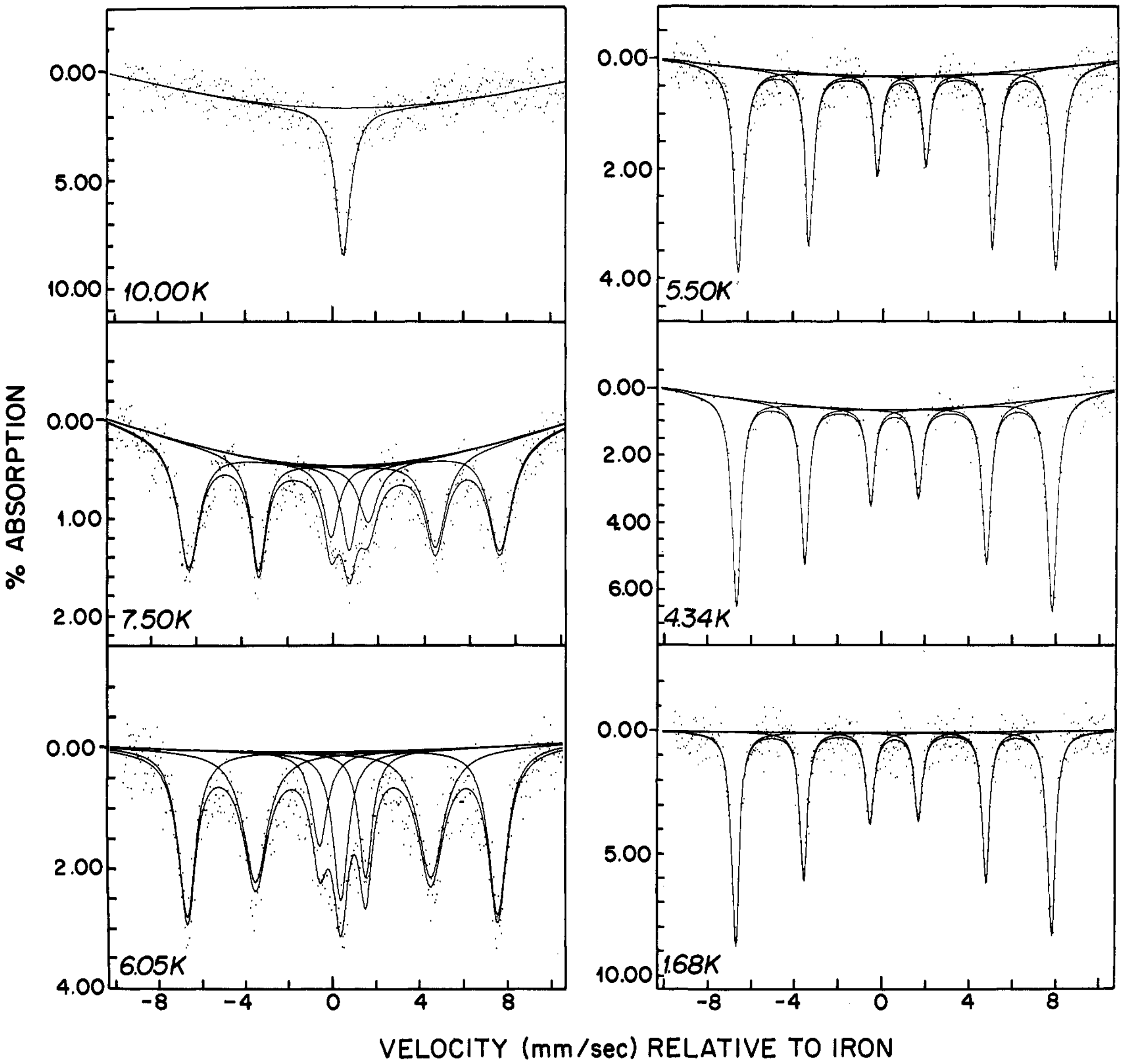

Figure 7. ^{57}Fe Mössbauer spectra of $[Fe(C_5Me_5)_2]^{\bullet+}[C_4(CN)_6]^{\bullet-}$ as a function of temperature for $1.68 \leq T \leq 10$ K.

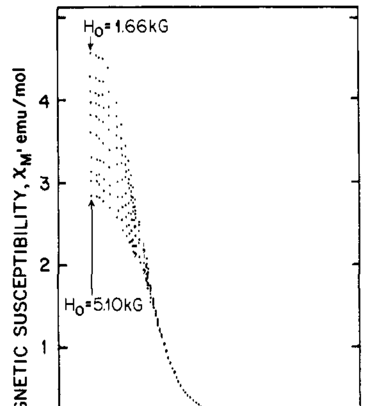

Figure 8. Field dependence of the molar magnetic susceptibility, χ_M vs. temperature, T, for $[Fe(C_5Me_5)_2]^{\bullet+}[C_4(CN)_6]^{\bullet-}$ for $1.66 \leq H \leq 5.10$ kG.

available to us using the SQUID susceptibility apparatus. This again indicates ferromagnetic as opposed to antiferromagnetic behavior. If the material does have the latter 3-D antiferromagnetic ground state, the critical field, H_c, must be small, i.e., <30 G. Finally, in Figure 10, we present isothermal magnetization, M, measurements at temperatures well above, below, and near the ordering temperature. The behavior is essentially as expected for an anisotropic 3-D ferromagnet, i.e., the magnetic moment varies linearly with H_0 for small H_0 above the ordering temperature and initially rises sharply with H_0 below the ordering temperature.

The saturation magnetization measured at 1.91 K and H_0 = 50 kG is 1.77 × 10^4 emu G/mol. This is greater than that observed for polycrystalline (1.1 × 10^4 emu G/mol)[5b] and oriented single-crystal (1.6 × 10^4 emuG/mol)[28] samples of $[Fe(C_5Me_5)_2]^{\bullet+}[TCNE]^{\bullet-}$ and even iron metal (1.2 × 10^4 emu G/mol).[5b] The high value for the magnetization is consistent with an $S = {}^1/_2$ anion and $S = {}^1/_2$ cation and a significant orbital contribution to the moment for the latter. Such an orbital contribution leads to single ion anisotropy (also for the ordered state) and is commonly observed for ferrocenium cations in a variety of environments.[5b,32,34]

---

(28) Chittapeddi, S. R.; Cromack, K. R.; Miller, J. S.; Epstein, A. J., submitted for publication.

(29) The coercive field[27] is microscopically related to domain wall movement and is the focus of further study.

(30) Thiel, R. E.; DeGraff, H.; DeJong, L. J. *Phys. Rev. Lett.* **1981**, *47*, 1415.

(31) The following diamagnetic corrections were used: $C_4(CN)_6$ = −162 × 10^{-6} emu/mol; $Fe(C_5Me_5)_2$ = −230 × 10^{-6} emu/mol;[4a] $Fe(C_5H_5)_2$ = −120 × 10^{-6} emu/mol.[32,33]

Table V. Weighted Least-Squares Planes for $[Fe(C_5Me_5)_2][C_4(CN)_6]$

	A	*B*	*C*	*D*
plane 1[a]	−0.9853	0.1676	−0.0323	−1.7228
atom	*x*	*y*	*z*	distance
		Atoms in Plane		
C1	1.8423	0.7949	0.6388	0.020 (10)
C2	1.6040	−0.4964	1.2473	0.019 (10)
C3	1.4792	−1.4925	0.2070	0.008 (10)
C4	1.6189	−0.8060	−0.0508	0.027 (10)
C5	1.8700	0.5953	−0.8020	0.006 (9)
C6	2.0700	2.0841	1.3613	−0.011 (12)
C7	1.5500	−0.7696	2.7443	−0.022 (11)
C8	1.2581	−2.9738	0.4041	−0.028 (12)
C9	1.5859	−1.4635	−2.4421	−0.006 (11)
C10	2.1268	1.6741	−1.8279	−0.033 (11)
		Other Atoms		
Fe	0.0000	0.0000	0.0000	1.723 (0)
		Atoms in Plane		
plane 2[a]	−0.9560	−0.2872	−0.0602	−1.5649
C11	0.0244	3.7153	7.3837	0.030 (11)
C12A	0.3504	2.5039	7.0835	0.085 (22)
C12B	0.1805	3.0316	8.5196	0.009 (23)
C13A	−0.1296	3.8614	9.0338	0.036 (21)
C13B	0.4190	2.7932	6.0679	−0.003 (19)
CN1	−0.1267	3.7470	9.953	10.011 (13)
CN2	−0.6528	2.1490	5.4695	−0.006 (11)
N2	0.8927	0.6227	8.6804	0.010 (11)
N3A	0.8886	1.8083	4.7422	−0.089 (19)
N3B	−0.1168	4.0255	10.7659	−0.127 (19)

χ^2 Values

plane no.	χ^2
1	36
2	95

Dihedral Angles = 26.4°

[a] The equation of the plane is of the form $Ax + By + Cz - D = 0$, where *A*, *B*, *C*, and *D* are constants and *x*, *y*, and *z* are orthogonalized coordinates.

Table VI. Average Intramolecular Bond Distances and Angles for $[C_4(CN)_6]^{z-}$ Compounds

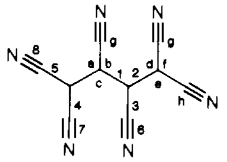

atoms	designation	$[C_4(CN)_6]^{\bullet-a}$ I	II	av	*cis*-$[C_4(CN)_6]^{2-b}$
CC—CC	1	1.43	1.43	1.43	1.399
C—CCC	2	1.29	1.33	1.31	1.436
$(C—CN)_{int}$	3	1.65	1.66	1.65	1.438
$(C_4—CN)_{endo}$	4	1.66	1.63	1.64	1.400
$(C_4—CN)_{exo}$	5	1.51	1.53	1.52	1.410
$(C\equiv N)_{int}$	6	0.93	0.91	0.92	1.147
$(C\equiv N)_{endo}$	7	0.84	0.86	0.85	1.157
$(C\equiv N)_{exo}$	8	1.093	1.093	1.093	1.160
C—C—CC	a	145	142	143	126.7
CC—C—CN	b	104	106	105	116.6
C—C—CN	c	110	111	110	116.5
$CCC—C—(CN)_{endo}$	d	118	120	119	121.9
$CCC—C—(CN)_{exo}$	e	116	112	114	119.7
NC—C—CN	f	126	128	127	118.2
$C—(C\equiv N)_h$	g	167 166	166 168	167	177.8
$C—(C\equiv N)_{exo}$	h	152	147	150	178.6
R, %				8.3	7.2
T, °C				−106	RT
ref			this work		21

[a] Planar. [b] Nonplanar.

Table VII. Mössbauer Parameters for $[Fe(C_5Me_5)_2]^{\bullet+}[C_4(CN)_6]^{\bullet-}$

temp, *T*, K	isomer shift[a] δ, mm/s	line width Γ, mm/s	internal field H_i, kG
1.68	0.507		449
4.34	0.508		448
5.50	0.517		434
6.50	0.488		430
7.50	0.509		423
8.50	0.508		417
10.00	0.502	0.80	
273	0.422	0.35	

[a] With respect to natural Fe foil.

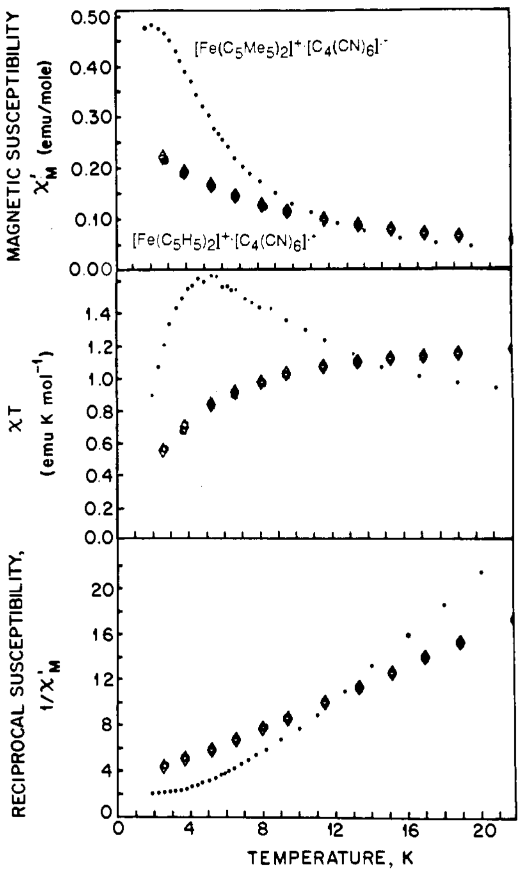

Figure 9. Molar magnetic susceptibility, χ_M vs. *T*, (top); χT vs. *T* (middle), and reciprocal magnetic susceptibility, χ_M^{-1} vs. *T*, for $[Fe(C_5Me_5)_2]^{\bullet+}[C_4(CN)_6]^{\bullet-}$ (30 G) and $[Fe(C_5H_5)_2]^{\bullet+}[C_4(CN)_6]^{\bullet-}$ (open symbols, 20.5, 16.4, and 12.4 kG) for $T < 20$ K.

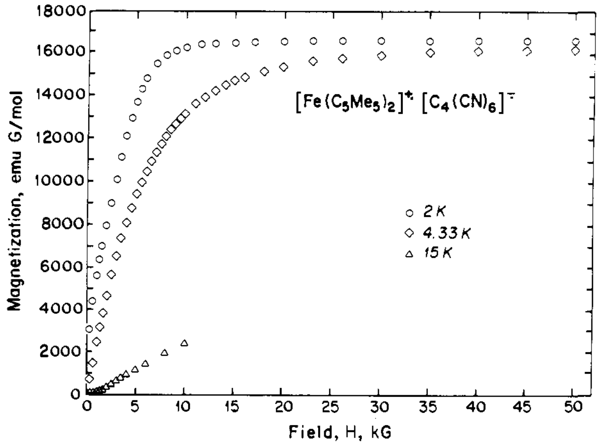

Figure 10. Field dependence of the magnetization, *M*(*H*), for $[Fe(C_5Me_5)_2]^{\bullet+}[C_4(CN)_6]^{\bullet-}$.

$[Fe(C_5H_5)_2]^{\bullet+}[C_4(CN)_6]^{\bullet-}$. In contrast the magnetic susceptibility of $[Fe(C_5Me_5)_2]^{\bullet+}[C_4(CN)_6]^{\bullet-}$ does not show evidence for ferromagnetic coupling. The susceptibility obeys the Curie–Weiss expression with $\theta = -3.4$ K and the effective moment, μ_{eff}, is 3.34 μ_B[35] (Figure 9). The moment vs. temperature variation is consistent with depopulation of the spin–orbit levels in a paramagnet and/or weak antiferromagnetic coupling. Similar behavior has also been reported for $[Fe(C_5H_5)_2]^{\bullet+}$ salts with diamagnetic anions, e.g., $[I]_3^-$ ($\theta = -1.33$ K)[36] and $[DDQ]^-$ ($\theta = -4.23$ K).[4b,32] Additionally, the susceptibility is essentially field independent and the low-temperature susceptibility plotted as χ^{-1} vs. T does not have an upturn to a constant value of χ^{-1} as noted for ferromagnetic $[Fe(C_5Me_5)_2]^{\bullet+}[C_4(CN)_6]^{\bullet-}$ and $[Fe(C_5Me_5)_2]^{\bullet+}[TCNE]^{\bullet-}$.[5,28]

Conclusion

We have shown that $[Fe(C_5Me_5)_2]^{\bullet+}[C_4(CN)_6]^{\bullet-}$ like $[Fe(C_5Me_5)_2]^{\bullet+}[TCNE]^{\bullet-}$ [5,28] possesses a 3-D ferromagnetic ground state. Both of these ferromagnetic charge-transfer complexes possess the same $\cdots D^{\bullet+}A^{\bullet-}D^{\bullet+}A^{\bullet-}\cdots$ structural motif; however other similarly structured complexes exhibit different magnetic behaviors, i.e., para- and metamagnetism. It seems clear that further studies are in order before we fully understand the specific structural/electronic features leading to a particular magnetic ground state in this class of compounds. This is particularly the case as substitution of $[Fe(C_5H_5)_2]^{\bullet+}$ for $[Fe(C_kMe_5)_2]^{\bullet+}$ although possessing the same electronic structure exhibits paramagnetic behavior. We attribute this to the latter salt belonging to a different structure type; however, crystals suitable for X-ray analysis have yet to be prepared. The structural determination of $[Fe(C_5H_5)_2]^{\bullet+}[C_4(CN)_6]^{\bullet-}$ should expand our knowledge of the structure–function relationship in this class of compounds.

Acknowledgment. W.M.R. and J.H.Z. gratefully acknowledge support from NSF DMR Solid State Chemistry Program Grant No. 8313710. We acknowledge the stimulating discussions with Prof. A. J. Epstein (Ohio State University) and Faraday susceptibility data for $[Fe(C_5H_5)_2]^{\bullet+}[C_4(CN)_6]^{\bullet-}$ taken by R. S. McLean (Dupont CR&DD).

Supplementary Material Available: Tables of the observed and calculated structure factors for $[Fe(C_5Me_5)_2]^{\bullet+}[C_4(CN)_6]^{\bullet-}$ (5 pages). Ordering information is given on any current masthead page.

---

[32] Hendrickson D. N.; Gray, H. B. *Inorg. Chem.* **1971**, *10*, 1559-1563.

[33] Rosenblum, M.; Fish, R. W.; Bennet, C. *J. Am. Chem. Soc.* **1964**, *86*, 5166-5170.

[34] Duggan, D. M.; Hendrickson, D. N. *Inorg. Chem.* **1975**, *14*, 955-970.

[35] Effective movements ranging from 2.8 to 4.4 have been observed. We attribute this to the orientational effects since the cation has $g_{\parallel} \sim 4.4$ and $g_{\perp} = 1.35$.[34]

A Transition-Metal Chromophore as a New, Sensitive Spectroscopic Tag for Proteins. Selective Covalent Labeling of Histidine Residues in Cytochromes *c* with Chloro(2,2′:6′,2″-terpyridine)platinum(II) Chloride

Eva Marie A. Ratilla, Herb M. Brothers II, and Nenad M. Kostić*

Contribution from the Department of Chemistry and Ames Laboratory of the U.S. Department of Energy, Iowa State University, Ames, Iowa 50011. *Received October 31, 1986*

Abstract: Reactivity and selectivity of $Pt(trpy)Cl^+$ toward proteins are studied with cytochromes *c* from horse and tuna as examples. The new transition-metal reagent is specific for histidine residues at pH 5. The reaction, facile one-step displacement of the Cl^- ligand by imidazole, produces good yield. The binding sites, His 26 and His 33 in the horse protein and His 26 in the tuna protein, are identified by UV–vis spectrophotometry and by peptide-mapping experiments. Model complexes with imidazole, histidine, histidine derivatives, and histidine-containing peptides are prepared and characterized. The covalently attached $Pt(trpy)^{2+}$ labels allow easy separation of the protein derivatives by cation-exchange chromatography. The labels do not perturb the conformation and reduction potential of cytochrome *c*, as shown by UV–vis spectrophotometry, cyclic voltammetry, differential-pulse voltammetry, EPR spectroscopy, and ^1H NMR spectroscopy. The selectivity of $Pt(trpy)Cl^+$ is entirely opposite from that of $PtCl_4^{2-}$ although both of them are platinum(II)–chloro complexes. Owing to an interplay between the steric and electronic effects of the terpyridyl ligand, the new reagent is unreactive toward methionine (a thio ether) and cystine (a disulfide), which are otherwise highly nucleophilic ligands, but very reactive toward imidazole, which is otherwise a relatively weak ligand. Unusual and useful selectivity of preformed transition-metal complexes toward proteins evidently can be achieved by a judicious choice of ancillary ligands. The strong UV and visible bands, some of them unobscured by the protein absorption, render the $Pt(trpy)^{2+}$ chromophore easy to detect and quantitate. The difference between the spectra of the tags bonded to His 26 and His 33 residues in the horse protein shows that the chromophore is sensitive not only to the nature of the binding site but also to its environment.

I. Introduction

Covalent modification of amino acid side chains has proved useful in studies of enzymes and proteins in general.[1-3] After many organic reagents have been developed, the promise of inorganic ones is becoming recognized. Various properties of transition metals render their complexes uniquely suited for labeling of biological macromolecules.[4,5] Charge-transfer absorption bands are strong and sensitive to the environment; paramagnetic ions serve as EPR probes and NMR relaxation agents; heavy metals are used as tags for X-ray crystallography and electron microscopy; binding selectivity can be controlled by the oxidation state, hardness or softness, coordination number, and charge.

---

[1] (a) Lundblad, R. L.; Noyes, C. M. *Chemical Reagents for Protein Modification*; CRC Press: 1984; Vols. I and II. (b) Means, G. E.; Feeney, R. E. *Chemical Modification of Proteins*; Holden-Day: 1971.

[2] Glazer, A. N. In *The Proteins*, 3rd ed.; Neurath, H., Ed.; 1977; Vol. 2, Chapter 1 and references cited therein.

[3] Sulkowski, E. *Trends Biotech.* **1985**, *3*, 1.

[4] Barton, J. K. *Comm. Inorg. Chem.* **1985**, *3*, 321 and references cited therein.

[5] *Metal-Ligand Interaction in Organic Chemistry and Biochemistry*; Pullman, B., Goldblum, N., Ed.; D. Reidel: Boston, 1977.

0002-7863/87/1509-4592$01.50/0